ELSEVIER

Surface and Coatings Technology 120–121 (1999) 663–667

SURFACE & COATINGS TECHNOLOGY

www.elsevier.nl/locate/surfcoat

Plasma immersion ion implantation into inner and outer races of industrial bearings

Z.M. Zeng [a,b], T.K. Kwok [a], X.B. Tian [a,b], B.Y. Tang [a,b], P.K. Chu [a,*]

[a] *Department of Physics and Materials Science, City University of Hong Kong, 83 Tat Chee Avenue, Kowloon, Hong Kong*

[b] *Advanced Welding Production & Technology National Key Laboratory, Harbin Institute of Technology, Harbin, People's Republic of China*

Abstract

Plasma immersion ion implantation (PIII) is a proven surface treatment technique and can be used to prolong the working lifetime of industrial components. However, the lateral implantation dose uniformity may not be very good, particularly for samples with an irregular shape. In this work, we focus on the PIII treatment of the inner and outer races of industrial bearings. The sheath expansion around the inner and outer races is simulated using a time-dependent, two-dimensional fluid model. The angular and spatial distributions of the incident ions along both the exterior and interior groove surfaces are derived. It is found that the ion dose is the highest on the bottom or center of the groove for both the inner and outer races. The minimum ion dose is near the corner of the groove as the ions impinge at a more glancing incident angle as a result of the ion-matrix sheath evolution. Compared with the exterior groove, the interior groove receives a smaller ion dose in the same implantation time. Our results also indicate that the spatial ion dose uniformity can be improved by reducing the implantation pulse width.

Keywords: Bearings; Plasma immersion ion implantation; Sheath simulation; Uniformity of implantation dose

1. Introduction

Plasma immersion ion implantation (PIII) is a proven technique for the surface modification of materials [1–4]. Because there is no line-of-sight restriction, it is an excellent technique to treat industrial components possessing an irregular shape. Moreover, as there are almost no dimensional changes during implantation, PIII is an effective means to enhance the surface properties of mechanical parts having strict dimensional tolerances such as precision bearings [5]. Consequently, it is the ideal last treatment process for industrial components. For a ball bearing assembly, the surface property of the balls can be improved by conventional beam-line ion implantation with good rolling manipulation or PIII. However, uniform implantation into the races of the inner and outer pieces is much more complicated because the working surfaces are not flat. In this work, a theoretical investigation is conducted to investigate the implant dose uniformity along the interior and exterior grooves shown in Figs. 1 and 2. It is aimed at formulating a theoretical model to simulate the sheath evolution in the vicinity of the industrial bearing as well as to identify the various factors influencing the PIII treatment process.

2. Model and simulation details

We base our work on a common industrial bearing (model 310) with an interior diameter of 50 mm as shown in Fig. 1. When the diameter of the piece and the width of the groove are more than the Debye length, we can assume that the component is initially uniformly filled with a charge-neutral plasma in which the density of electrons and ions are both n_0 and the potential ϕ is initially zero everywhere. At time $t=0$, the sample potential is switched from $\phi=0$ to a negative potential $\phi=\phi_t$ to induce the formation of an ion-matrix sheath. The electrons are repelled from the target and ions are initially at rest for the ion mass is much larger than the electron mass. When $t>\omega_{pe}^{-1}$ (inverse electron plasma frequency), ions are accelerated by the electric field and implanted into the target until the applied voltage pulse

* Corresponding author. Tel.: +852-2788-7724; fax: +852-2788-9549.

E-mail address: paul.chu@cityu.edu.hk (P.K. Chu)

0257-8972/99/$ – see front matter
PII: S0257-8972(99)00433-8

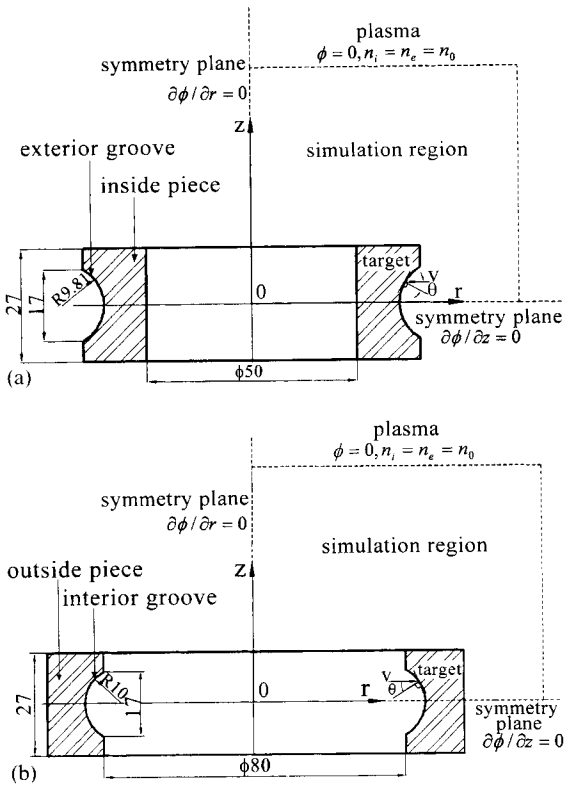

Fig. 1. Dimensions (mm) and simulated regions of the (a) inner piece and (b) outer piece of a bearing.

is over. The evolution of the ion density n_i, ion velocity v_i, and potential ϕ can be modeled using cold, collisionless fluid ions, Boltzmann electrons and Poisson's equation [6–11]. In cylindrical coordinates, the two-dimensional equations of ion continuity and motion, Poisson's equation and Boltzmann relation are:

$$\frac{\partial n_i}{\partial t}+\frac{1}{r}\frac{\partial}{\partial r}(rn_iv_{ir})+\frac{\partial}{\partial z}(n_iv_{iz})=0 \tag{1}$$

$$\frac{\partial v_{ir}}{\partial t}+v_{ir}\frac{\partial v_{ir}}{\partial r}+v_{iz}\frac{\partial v_{ir}}{\partial z}=-\frac{e}{m}\frac{\partial\phi}{\partial r} \tag{2a}$$

$$\frac{\partial v_{iz}}{\partial t}+v_{ir}\frac{\partial v_{iz}}{\partial r}+v_{iz}\frac{\partial v_{iz}}{\partial z}=-\frac{e}{m}\frac{\partial\phi}{\partial z} \tag{2b}$$

$$\frac{1}{r}\frac{\partial}{\partial r}\left(r\frac{\partial\phi}{\partial r}\right)+\frac{\partial^2\phi}{\partial z^2}=-\frac{e}{\epsilon_0}\left[n_i-n_0\exp\left(\frac{e\phi}{KT_e}\right)\right] \tag{3}$$

where e is the charge (it is assumed that the ions are singly charged) and m is the ion mass. It is noted that the Bohm sheath criterion, pre-sheath requirements, matrix sheath, and steady state Child Law sheath are basically derived from ion continuity and Poisson's equations [12]. Therefore, the fluence of ions accelerated in the pre-sheath towards target and ions uncovered by the expanding sheath is already considered by numerically solving the dynamic two-dimensional equations [Eqs. (1)–(3)]. It is more convenient to make Eqs. (1)–(3) dimensionless by introducing the following variables:

$$R=x/s_0,\ Z=z/s_0,\ \psi=\phi/\phi_t,\ n=n_i/n_0,\ u_R=v_{ir}/v_{max},\ u_Z=v_{iz}/v_{max},\ \tau=t\omega_{pi} \tag{4}$$

where $s_0=\sqrt{-2\epsilon_0\phi_t/en_0}$ is the planar ion ion-matrix sheath width, $v_{max}=\sqrt{-2e\phi_t/m}$ is the velocity that an ion would gain if it fell through a potential drop ϕ_t, and $w_{pi}=\sqrt{n_0e^2/\epsilon_0m}$ is the ion plasma frequency. The equations become:

$$\frac{\partial n}{\partial\tau}+\frac{1}{R}\frac{\partial}{\partial R}(Rnu_R)+\frac{\partial}{\partial Z}(nu_Z)=0 \tag{5}$$

$$\frac{\partial u_R}{\partial\tau}+u_R\frac{\partial u_R}{\partial R}+u_Z\frac{\partial u_R}{\partial Z}=\frac{1}{2}\frac{\partial\psi}{\partial R} \tag{6a}$$

$$\frac{\partial u_Z}{\partial\tau}+u_R\frac{\partial u_Z}{\partial R}+u_Z\frac{\partial u_Z}{\partial Z}=\frac{1}{2}\frac{\partial\psi}{\partial Z} \tag{6b}$$

$$\frac{1}{R}\frac{\partial}{\partial R}\left(R\frac{\partial\psi}{\partial R}\right)+\frac{\partial^2\psi}{\partial Z^2}=2\left[n-\exp\left(\frac{e\phi_t}{KT_e}\psi\right)\right]. \tag{7}$$

The simulation regions for the interior and exterior grooves are depicted in Fig. 1(a) and (b). The initial conditions are $n=1$ and $u_R=u_z=0$ everywhere. The boundary conditions are $\psi=1$ on the target, $\psi=0$ in the plasma, $\partial\psi/\partial r=0$ at the central symmetry axis, and $\partial\psi/\partial z=0$ on the lower boundary because it is the symmetry plane of the target.

The equations can be solved by the finite difference method. The simulation parameters are selected to reflect typical PIII conditions: $n_0=3.5\times10^9\,cm^{-3}$, $\phi_t=-20$ kV, $kT_e=1.5$ eV, and N_2^+ plasma, and consequently, $s_0=25.1$ mm and $\omega_{pi}^{-1}=0.0678$ μs. We choose a grid spacing $h=\Delta R=\Delta Z=1/32\ s_0=0.784$ mm and a time step of $\Delta\tau=1/64$. The simulation region is chosen to be $6s_0=15.06$ cm in height and $8s_0=20.08$ cm in the radial direction, so that the sheath will remain inside it throughout the entire simulated time duration. The simulation is conducted to a final step $\tau=100$ ($t=6.78$ μs). According to the implantation condition, the Child Law sheath is 15.14 cm. At $\tau=80$, i.e. $t=5.42$ μs, the dynamic sheath has expanded to around $3s_0=7.53$ cm from the bearing (see Section 3). Therefore, the total simulation time is smaller than the duration of a supersonic sheath expansion. Since the arc boundary of the groove is a curved surface, not all of the boundary grid points are exactly on the target boundary. Hence, the values of the boundary grid points along the groove are calculated by linear interpolation with an error of 0 (h^2).

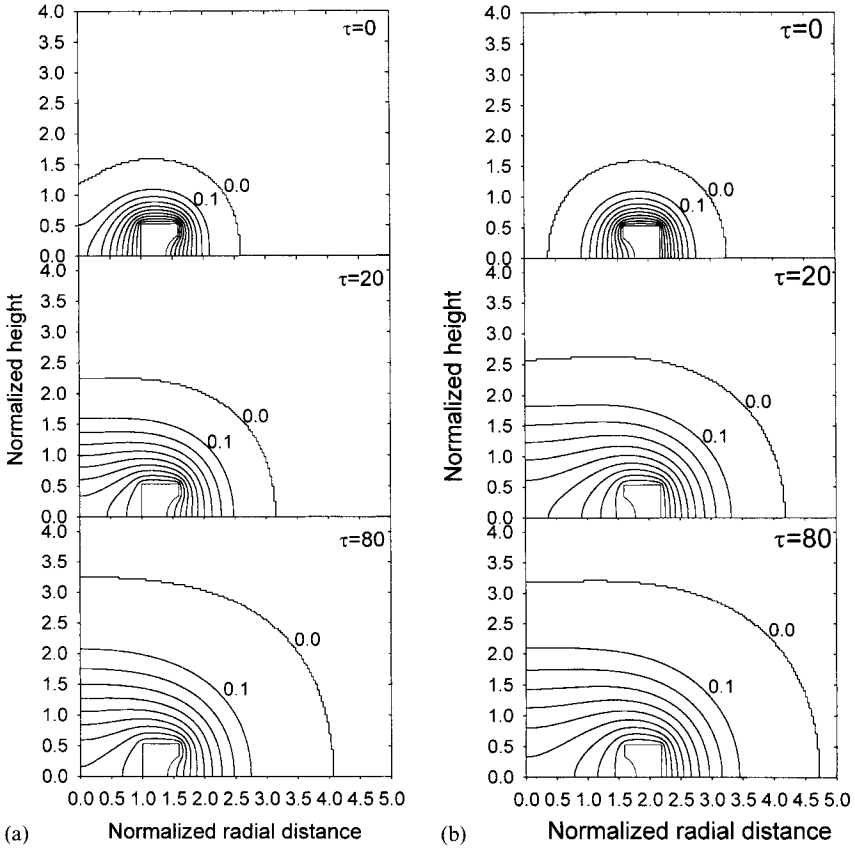

Fig. 2. Evolution of the normalized potential contour lines around the (a) inner piece and (b) outer piece of a bearing.

3. Results and discussion

The temporal evolution of the potential contour lines around the exterior and interior grooves is shown in Fig. 2(a) and (b) for $\tau=0$, 20 and 80. At $\tau=0$, it shows the potential distribution of the ion-matrix sheath. For the exterior groove, the interior radius of the inside piece is equal to s_0, and so the ion-matrix sheath has overlapped in the center. However, for the interior groove of the outer piece, the ion-matrix sheath has not overlapped because its interior radius is about $1.6s_0$. According to Sheridan [13,14], the ion-matrix overlap radius s_1 in a cylindrical bore is $\sqrt{2}s_0$. Therefore, our results are consistent. As the sheath propagates, the conformality of the potential contour with the target surface degrades, and when $\tau=80$, the field lines have almost taken a dome shape for both the exterior and interior grooves.

The working surfaces are the arc grooves on which the balls roll. Hence, we only need to derive the results on the two groove surfaces. Fig. 3(a) and (b) display the temporal evolution of the ion density around the two grooves. As shown in Fig. 3(a), the ions within the race are almost depleted when $\tau=20$, but this does not affect the implantation into the exterior groove. Hence, the exterior groove undergoes implantation at all times. On the other hand, according to Fig. 3(b), implantation into the interior groove of the outer piece does not fare as well as the number of ions within the race becomes less with time. At $\tau>20$, the ions within the race are almost exhausted. When $\tau=80$, only a few ions originating from above the sample impinge into the interior groove surface, and there is minimal implantation.

Fig. 4 depicts the distribution and temporal evolution of the ion incident angle relative to normal (for the groove, the normal direction is the radial direction). For the exterior groove on the inner piece shown in Fig. 4(a), ions strike the area near the groove corner (or edge) at a glancing angle. Initially, the angle of incidence along the groove surface has small values (relative to normal). As the sheath expands, the incident angle becomes more oblique, except near the center of the groove. When $\tau=20$, the incident angle at the groove corner reaches nearly 70°. At a later time, ions impinge nearly parallel to the surface, thereby resulting in more sputtering than implantation near the corner. For the interior groove of the outer piece [Fig. 4(b)], the incident angle near the groove corner is also larger than that at the groove bottom or center. The incident angle along the groove surface is small in the beginning, but increases rapidly with time. For instance, when $\tau=10$, the incident angle near the groove corner has reached 90°. Hence, after

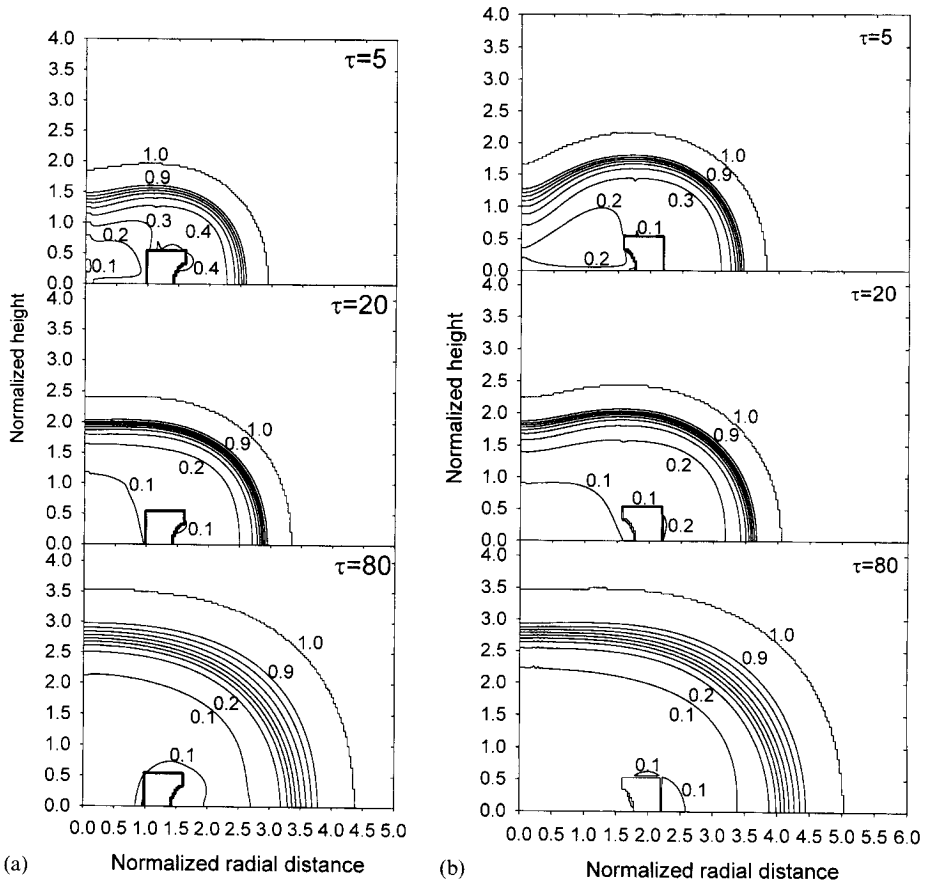

Fig. 3. Evolution of the normalized ion density contour lines around the (a) inner piece and (b) outer piece of a bearing.

that, there is very little implantation near the groove corner. As the sheath expands, a larger area of the groove experiences glancing ion implantation. In fact, when $\tau > 50$, the incident angle at the groove center is larger than 60° and the implantation efficiency is quite low. It can thus be inferred that a longer implantation pulse does not necessarily increase the implantation dose.

The incident ion dose $D(r, z)$ can be calculated by integrating the ion flux into the target surface:

$$D(r,z)=\int_0^{t_p} n_i(t,r,z)v_{i\perp}(t,r,z)\,dt=\int_0^{t_p} n_i(t,r,z)\sqrt{v_{ir}^2(t,r,z)+v_{iz}^2(t,r,z)}\cos\theta\,dt \quad (8)$$

where t_p is the pulse duration and $v_{i\perp}$ is the ion velocity normal to the target surface. The results are exhibited in Fig. 5. A larger ion dose is observed near the groove center compared to the edge for both the exterior and interior grooves. When $\tau = 20$, the ion implant dose is quite uniform along both groove surfaces. However, as the pulse time increases, it begins to deviate because of the larger incident angle near the groove. Comparing Fig. 5(a) and (b), the ion dose along the exterior groove is more uniform than that on the interior groove. In addition, for the same pulse duration, a higher ion dose is implanted into the exterior groove. For the interior groove on the outer piece, the ions within the piece are depleted quickly. The ions coming from the top or other half have a large vertical (z-direction) velocity component and very few of them are implanted into the groove. This explains why the interior groove of the outer piece has a smaller ion dose than the exterior groove of the inner piece. Hence, if a high dose into the interior groove is intended, the total implantation time must be longer. In addition, a shorter pulse duration yields better spatial uniformity.

4. Conclusion

Our results reveal ion dose variation along the working surface of the outer and inner pieces of a ball bearing. In both the exterior and interior grooves, the maximum ion dose is achieved near the bottom or center

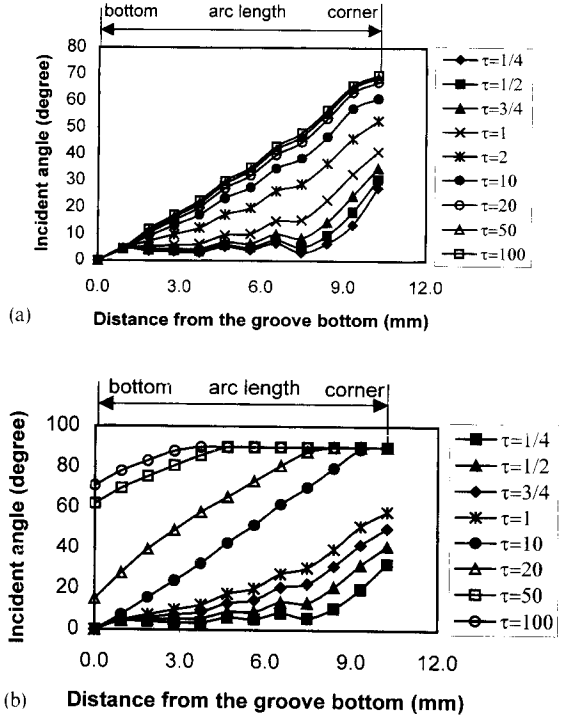

Fig. 4. Variation of the incident angle distributions (from normal) along the groove surface with time for the (a) exterior groove of the inner piece and (b) interior groove of the outer piece.

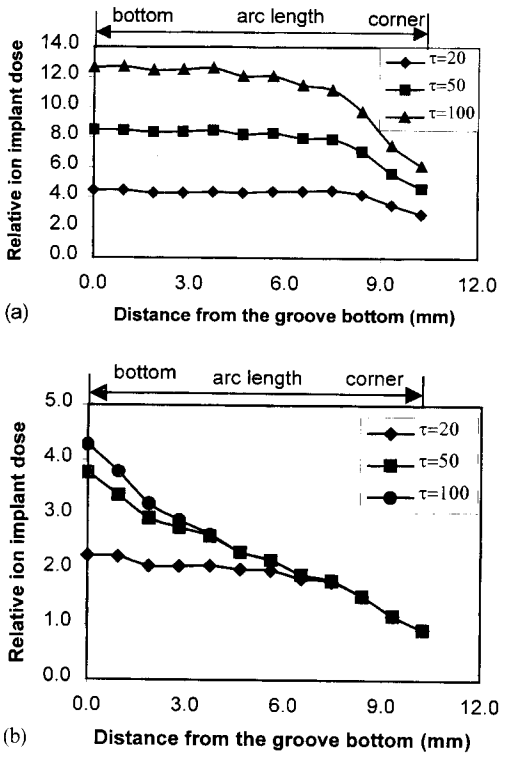

Fig. 5. Relative ion implant doses along the surface of the (a) exterior groove of the inner piece and (b) interior groove of the outer piece.

of the arc groove and the minimum dose is observed near the corner. This is due to ions bombarding at a more glancing angle near the edge as a result of the evolution of the ion sheath. Under the same PIII conditions, the exterior groove of the inner piece receives a higher dose and better uniformity compared to the interior groove of the outer piece of the bearing. This shows that the PIII treatment of the interior groove is more difficult. A longer total implantation time is needed. Our data also suggest that shorter implantation pulses will yield more uniform implantation along the grooves of industrial ball bearings.

Acknowledgement

This work is supported by the Hong Kong Research Grants Council Earmarked Grants 9040332 and 9040344.

References

[1] J.R. Conrad, J.L. Radtke, R.A. Dodd, F.J. Worzala, N.C. Tran, J. Appl. Phys. 62 (1987) 4591.
[2] J.R. Conrad, R.A. Dodd, S. Han, M. Madapura, J. Scheuer, K. Sridharan, F.J. Worzala, J. Vac. Sci. Technol. A 8 (1990) 3146.
[3] B.Y. Tang, Physics 23 (1994) 42.
[4] S.Y. Wang, P.K. Chu, B.Y. Tang, X.C. Zeng, X.F. Wang, Nucl. Instrum. Meth. B 127 (1997) 100.
[5] M. Hirano, S. Miyake, Appl. Phys. Lett. 49 (1986) 779.
[6] M. Windner, I. Alexeff, W.D. Jones, K.E. Lonngren, Phys. Fluids 13 (1970) 2532.
[7] T.E. Sheridan, M.J. Alport, J. Vac. Sci. Technol. B 12 (1994) 897.
[8] T.E. Sheridan, J. Phys. D: Appl. Phys. 29 (1996) 2725.
[9] M. Hong, G.A. Emmert, J. Vac. Sci. Technol. B 12 (1994) 889.
[10] M. Hong, G.A. Emmert, J. Appl. Phys. 78 (1995) 8967.
[11] T.E. Sheridan, Appl. Phys. Lett. 64 (1994) 1783.
[12] M.A. Lieberman, A.J. Lichtenberg, Principles of Plasma Discharges and Materials Processing, Wiley, New York, 1994. Chapter 6.
[13] T.E. Sheridan, J. Appl. Phys. 74 (1993) 4903.
[14] T.E. Sheridan, J. Appl. Phys. 80 (1996) 66.